

11 November 2013

**Report to Prince William Sound Citizen's Regional Advisory Council:
Future Iceberg Discharge from Columbia Glacier, Alaska**

Reference PWSRCAC Project #8551

Contractor: W. T. Pfeffer Geophysical Consultants, Nederland, Colorado

Report #3

1. Introduction

Report #3 to PWSRCAC for FY13 consists of two main parts. In part one (Updates), we provide topic-focused progress updates for each component of our ongoing research, drawing on information derived from our time lapse cameras and a variety of remote sensing products. We also use newly available information, both unpublished and in the peer-review scientific literature, including a new paper (Rignot et al, 2013) containing airborne radioecho sounding measurements of ice thickness in the Columbia Glacier East Branch. In part two (Synthesis), we assess all available data and analysis to evaluate the current status of the retreat and make a refined estimate of future retreat, calving, downfjord ice transport, and passage of ice over the Heather Bay Moraine Shoal. While further analysis remains to be done, we are now at a stage where can make qualitative assessments of future retreat, calving, and iceberg transport at a fairly high level of confidence. This assessment appears at the end of this report.

2. Updates: Icebergs at Heather Bay Moraine Shoal, Iceberg transport from Columbia Glacier terminus to moraine shoal, Calving at present terminus, Glacier flow dynamics.

2a. Heather Bay Moraine Shoal (HBMS)

Observations and analysis at HBMS are oriented at understanding how icebergs behave on entering the shallow water approaching HBMS from its landward side, under what conditions bergs are able to pass over the shoal and into the open waters on the seaward side of the shoal, and to characterize or place limits on the size distribution of bergs entering Prince William Sound proper. In report 2, we established that the geometry of HBMS is essentially stable: portions of the moraine have experienced minor erosion and deposition, but few changes exceed the precision of the existing measurements. The obstacle presented to bergs by the moraine itself is thus assessed to be constant over time.

For observation of iceberg behavior at and near HBMS we rely on three principal data sources:

1) High-frequency time-lapse monitoring of HBMS, which began in May, 2013, and has so far provided a continuous 20-minute interval image sequence during daylight hours. Image data was retrieved on 19 September 2013. The camera has been left operating and will be serviced again in late winter 2014. A sample sequence from this camera is included on a flash drive with this report, and is also temporarily posted at [http://ftpext.usgs.gov/pub/wr/ak/anchorage/ONeel/Heather island](http://ftpext.usgs.gov/pub/wr/ak/anchorage/ONeel/Heather%20island)

2) High-frequency time-lapse monitoring of the lower glacier, from a camera position (camera AK-10) ca. 3 km upstream from the present terminus. The synchronized observations of iceberg production at the glacier terminus and iceberg arrival at HBMS provide constraints on the speed of iceberg transport and berg degradation during downfjord transport.

3) Satellite imagery analysis of glacier motion and of icebergs in the forebay reach between the glacier terminus and HBMS. Imagery from the German TerraSAR-X satellite has high spatial resolution (ca. 1-3 m) and is repeated every 11 to 22 days. Velocity and strain rate fields are obtained by SAR-interferometric methods, providing us with detailed views of changing ice flow conditions in the glacier channel and repeated views of icebergs in the forebay reach, from which iceberg size distributions may be extracted by standard image processing methods.

The HBMS camera operated without failure from May through September, 2013, capturing over 6000 images, and has been left in place to shoot throughout the 2013/14 winter. Ice volume on the inside of the moraine is highly variable, and while the density of icebergs is less than in recent years (and far less than in the first ca. decade of the retreat), occasional large bergs continue to be delivered to the moraine. We expect that three factors work to reduce the mean iceberg size at HBMS in recent years: these are 1) increasing distance from the source of icebergs to HBMS as the terminus retreats, 2) smaller initial berg size on calving, since the mean terminus ice thickness has been reduced upon regrounding in shallow water in the Main Branch (ca. summer, 2010), immediately upstream of Juncture and 3) warmer waters in the forebay, which accelerate iceberg melt rates. Warmer waters are partly the result of inflow of warming waters from Prince William Sound and partly due to reduction in iceberg density in the forebay, which allows faster solar heating of surface waters. These factors affect all icebergs traversing the forebay from the glacier terminus to HBMS, but large bergs are still occasionally calved, and under favorable conditions survive the journey to HBMS without losing a great deal of mass.

The presence of larger icebergs at HBMS is important for the impoundment of ice inside the shoal, because the larger grounded bergs present obstacles to the passage of

smaller bergs that might otherwise pass over the shoal on a high tide. We hypothesize that the absence of large bergs near HBMS may be a factor in the occasional flushing of icebergs from most or all of the forebay, an event first recorded in 1996 and documented occasionally during the IMP1 project. We have not yet identified the mechanism responsible for the flushing events, but the candidate processes include tides, currents in the forebay, water temperature, winds, calving rate, and initial berg size distribution on calving.

As large icebergs that arrive at HBMS melt and fracture, the size distribution of bergs as determined by direct measurements at points along the forebay may be altered significantly. Once grounded, large icebergs are more strongly influenced by tidal forcing than a floating berg. As the tide level changes, the center of gravity of grounded berg shifts, rotating the berg and generating stresses that can fracture it into smaller pieces. A good example of this is visible in the supplied time lapse sequence, between 23 and 25 July, in the center of the field of view. In addition to fracture, rotation of the berg over several tidal cycles can “jack” the berg up the slope of the landward side of the shoal, possibly allowing it to escape into Prince William Sound despite being far too large to be simply floated over the shoal. (The occasional presence of anomalously large icebergs on the seaward side of HBMS suggests that this, or some comparable process, must be occurring.) Submarine melt rates also increase during these grounding episodes due to tidal friction arising from accelerated flow around the iceberg in shallow water.

Our scheme for quantifying submarine melt rates is not yet implemented, but the imagery nevertheless demonstrates that subaerial melt rates are large. In the 23 July grounding events, the grounded berg is noticeably smaller towards the end of the grounding episode. Fracture and melting evidently work in concert to reduce berg size, eventually producing berg fragments small enough to float over HBMS on a sufficiently high tide. In the future, we will be able to use time lapse sequences from Heather Island and camera AK10 (Figure 1) to investigate relationships between iceberg production at the calving terminus and iceberg densities at HBMS. We do not presently know if episodes of calving travel coherently downfjord to the shoal, or if intermediate processes divert and retard some bergs while accelerating others.

2b. Downfjord ice transport

Since early summer, we have been developing image processing methods (such as binary contrast stretching and edge detection) to quantify iceberg size distributions at positions along the forebay. Once completed, a robust and efficient image processing workflow will allow us to extract iceberg size distributions from more than 50 TerraSAR-X images acquired since 2011. A second key goal is to estimate iceberg residence time (travel time from calving to arrival at HBMS), but tracking individual icebergs as they

move over the entire ca. 20 km path is proving to be a challenge, due to the spatial limitations of our ground-based time lapse photography and temporal limitations of the TerraSAR-X imagery.

2c. Observations and analysis of calving at present terminus

Sarah Neuhaus, a PhD student at UC Santa Cruz, assisted in the image processing development described above during the summer of 2013, working as a USGS intern supervised by Shad O'Neel. Neuhaus also analyzed time lapse image sequences from camera AK10 (Figure 1) that capture berg motions in the immediate vicinity of the glacier terminus. Iceberg grounding in the immediate vicinity of the terminus can be seen in the imagery, and confirms that newly exposed shallows provide opportunities for bergs to become grounded shortly after calving. Trapping of larger icebergs by grounding in the shoals near the glacier terminus skews the size distribution of bergs leaving the terminus region relative to the size distribution of calved bergs. One unexpected discovery from this time lapse series is the observation that icebergs tend to ground near or shortly below high tide, rather than at low tide. Apparently larger icebergs drift furthest into the shoals near the glacier margins at high tide, and ground as the tide starts to fall. Large bergs also tend to become ungrounded faster than medium and small sized bergs, in part due to their tendency to roll and break up rapidly upon grounding.



Figure 1. View from camera AK10 looking downstream toward Columbia Bay. Locations of iceberg grounding events during summer 2012 are color-coded by size, showing the newly revealed shallow locations in the proximal regions of the fjord. Camera AK10 is maintained through a partnership between the Extreme Ice Survey, WT Pfeffer Geophysical Consultants, and the USGS.

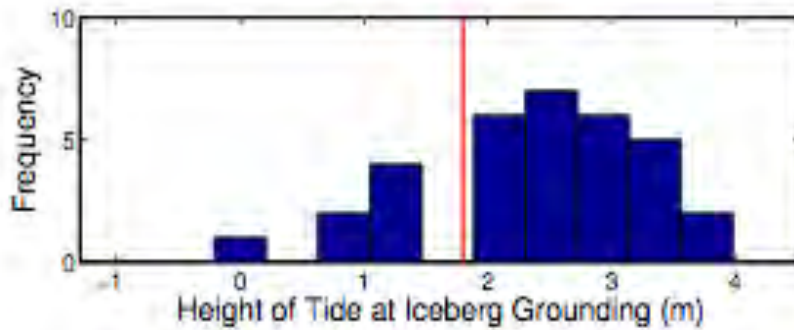


Figure 2. Histogram showing tide height at onset of iceberg grounding events, demonstrating that icebergs tend to drift into otherwise impassable regions during high tide and subsequently become grounded.

2d. Upstream dynamics, future retreat and calving.

When the glacier terminus position is relatively stable over time, as has been the case at Columbia Glacier since summer 2010, changes in flow speed translate directly into changes in calving rate (Figure 3 and Meier and Post, 1987).

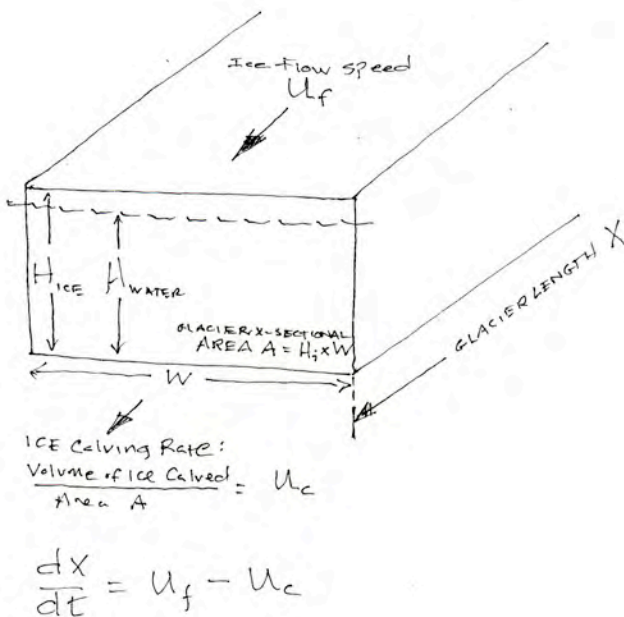


Figure 3. Schematic showing relationship between glacier terminus position, ice flow speed, and calving rate.

Evaluation of the glacier ice flux (volume or mass per unit time pass a reference point on the glacier) requires a complete glacier geometry at a “flux gate” or cross-section of the glacier, as well as a profile of ice motion and measurement or assumption about the variation of flow speed with depth. We define two flux gates, just upstream of the Main and West branch termini (Figure 4). Ice motion at these gates is determined from TerraSAR-X interferometry, using radar data acquired on a nominal 11-day repeat cycle between January 2011 and June 2013. Georectified digital elevation models (DEMs) were calculated from Worldview satellite stereo-pairs collected during 2012. These DEMs, together with swath LiDAR profiles collected by University of Alaska’s NASA Icebridge Mission, constrain the changing surface elevation of the near-terminus region, but on different time steps than the TerraSAR-X-derived velocity is measured. We interpolate the surface elevation change record to common times by linearly fitting the rate of elevation change, applied to the average surface profile geometry. The bed is resolved with a highly data-constrained model (McNabb et al., 2012). We calculate flux as the integrated product of velocity and thickness in 100 m wide cells spanning the entire terminus width, then plot them as a function of time (Figure 5).

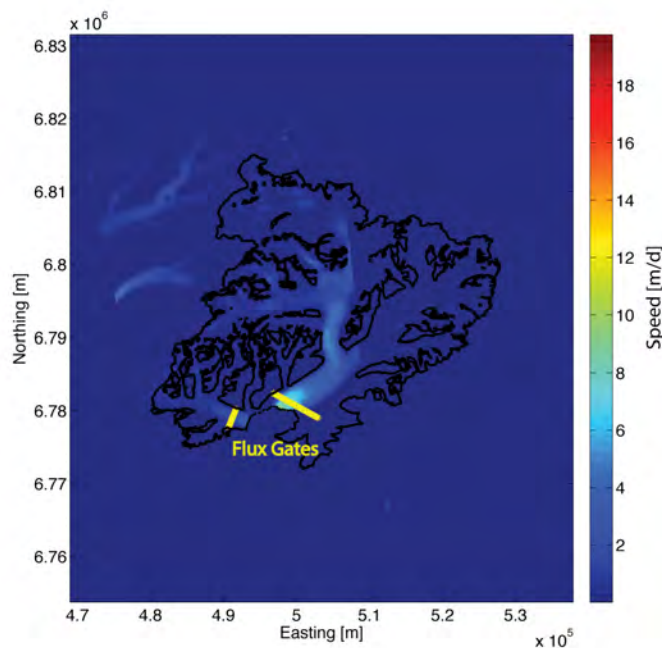


Figure 4. Example of TSX velocity field with Columbia Glacier outline and flux gates overlaid.

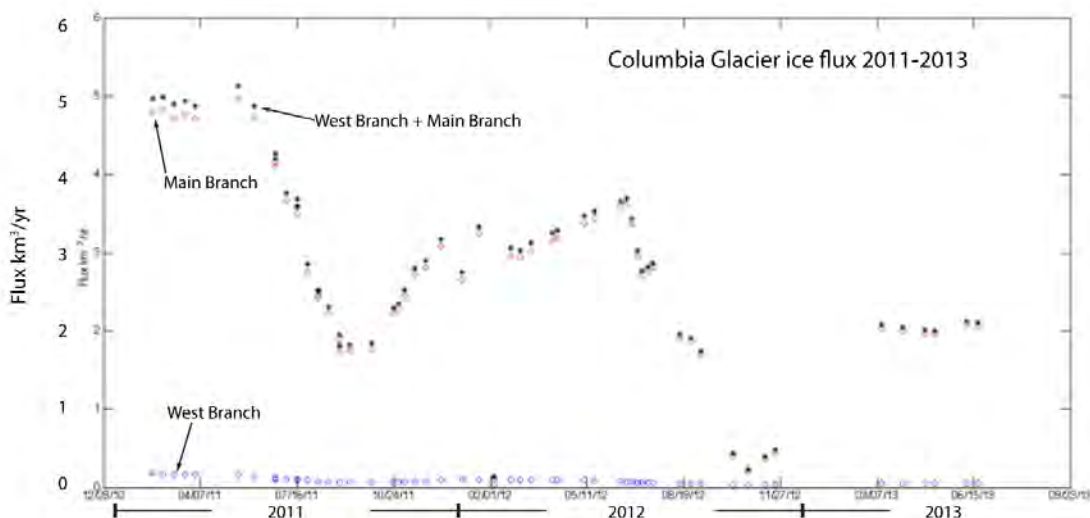


Figure 5. Ice flux (m^3/yr) to the terminus as a function of time (January 2011 through June 2013). Blue circles are from the west branch, red from the main branch, and black stars represent the sum of the two branches.

Average ice flux from both the Main and West branches of the glacier averaged $2.23 \text{ km}^3/\text{yr}$ from late 2010 to the present (late 2013), with virtually all of the flux coming from the Main branch. (The West branch terminus retreated to very shallow water in ca. 2009, and is in addition fed by a much smaller catchment than the Main branch.) Seasonal variability is apparent at ca. $1.0 \text{ km}^3/\text{yr}$, or ca. 45% of the mean flux, superimposed on a secular decreasing trend in flux. This trend is a continuation of the decline in flux observed following a maximum of ca. $7 \text{ km}^3/\text{yr}$ in the early-mid 2000s as the glacier's terminus entered the deep basin at the West/Main branch confluence. Seasonal variability is characterized by a slow increase in flux during fall through spring, peaking in early summer and falling rapidly to a minimum in late summer.

The sparseness of observations before the TerraSAR-X era (and after the withdrawal of support for regular, multi-annual aerial photogrammetric missions) led to possible under-estimates of ice flux in the mid-2000s (e.g. O'Neel et al, 2005) since the photo missions flown at that time were generally in mid-late summer, when the flux would have been at or near a seasonal low, and no other information existed to apply a seasonal correction.

Short-term (sub-annual) variability in ice flux is primarily forced by speed variations coincident with changes in basal hydraulics (Meier et al, 1994; Kamb et al, 1994). In contrast, the secular trend of reduced flux is a result of thinning of the glacier, which reduces both speed and cross-sectional gate area. Short-term speed variations are coherent over much longer length scales (e.g. high on the Main branch and on tributaries) than stress-coupling theory permits (Kamb and Echelmeyer, 1986a,b; Echelmeyer and Kamb, 1986), implying that ice dynamics are strongly modulated by basal hydrology, the only process available to couple flow dynamics over such long

length scales. Seasonal and shorter time scale changes in motion exhibit maximum variability at the terminus, and decay rapidly upstream.

Comparison with the Krimmel (2001) analysis shows that the timing of seasonal variations in speed is roughly consistent over the history of the retreat. There have been occasional periods during the retreat when the seasonal variation in flux may have diminished or vanished altogether, but the timing of observations has been too sparse at various times during the retreat for these to be interpreted with any confidence. Through the TerraSAR-X era, peak speeds occur *ca.* 2 months later in the year than early in the retreat, but minimum speeds have not shifted in time. Variability in flow speed appears to be fairly consistent over the course of the retreat when measured relative to the terminus position, *i.e.* measured at a position that follows the retreating terminus at a fixed distance (e.g. *ca.* 10 km upstream). The combined effect of these changes is that discharge has become more variable. Indeed, time-lapse imagery and velocity fields both demonstrate that some of the slowdowns nearly stop the ice motion altogether. These slowdowns may be a factor in the occurrence of ice-free forebay conditions.

Our results agree with the conclusions of McNabb et al. (2012), namely, that current discharge rates have fallen significantly since the mid-2000s when the glacier was changing most rapidly. The position of the terminus since *ca.* 2009 lie outside of the region covered by earlier photogrammetric surveys, so there is no single location where ice flux can be monitored over the entire course of the retreat. However, we can compare migrating near-terminus flux estimates, as described above, to confirm that the discharge flux is declining over time.

The drawdown of the Columbia Glacier reservoir is so considerable that *extended* episodes (> 1 year to decades) of high-volume ice discharge is unlikely in the future. Newly acquired airborne radar results (Rignot et al., 2013) show an overdeepening in the East branch channel some 18 km upstream from the present terminus (Figure 6). This basin comprises a *ca.* 5 km-long marine-grounded reach of ice lying as much as 300 m below sea level. The basin lies some 2 to 4 km upstream from the originally anticipated upglacier limit of retreat, which was defined as the upstream limit (as determined before the publication of Rignot et al., (2013) of marine-grounded ice.

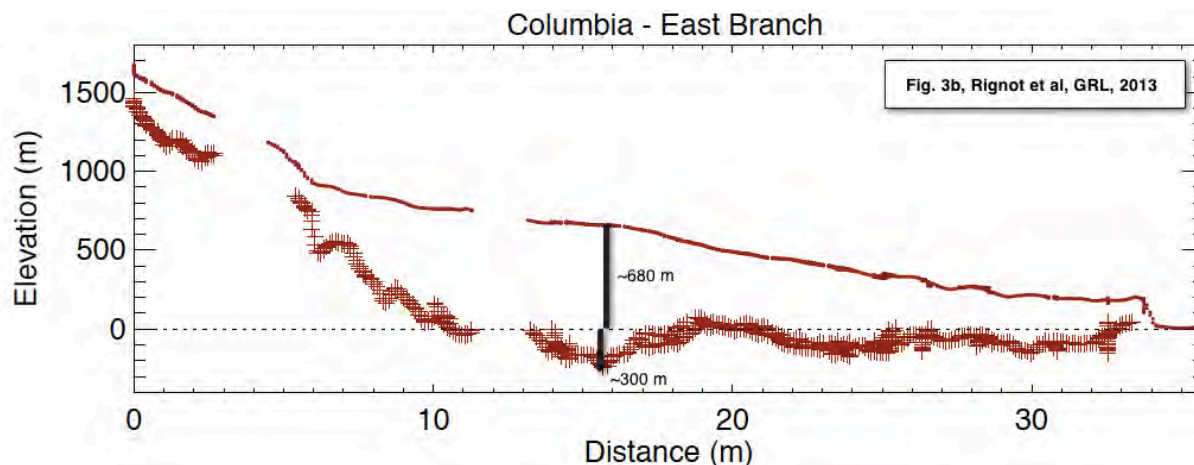


Figure 6. Along-flow profiles of surface elevation and basal topography at the East Branch of Columbia Glacier (from Rignot et al, 2013)

This basin may result in an extension of the glacier’s retreat into the East branch for several years, as well as some interval of accelerated flow and increased calving. The timing of terminus retreat into this basin, and duration and magnitudes of accelerated flow and calving during the traverse of the terminus across the basin, are poorly constrained at this time, but several factors suggest that the response of the glacier to this overdeepening may not be large in magnitude or long in duration. These factors include a bedrock sill near or slightly above sea level at the downstream limit of the basin (at km 18-21 in Figure 6) and the fact that at 300 m depth, this basin is comparatively shallow. Further soundings are required to map the lateral extent of the sill; if there is continuous shallow barrier extending across the entire glacier channel, then the retreat will not easily be able to propagate beyond and into the basin. Furthermore, while the ice over the basin at present is very thick (ca. 1000 m), significant thinning will likely have occurred by the time the terminus reaches the basin, and conditions may be similar to conditions today, with modest calving rates.

The overdeepened basin may potentially extend the duration of retreat, and produce some brief (2 year or less) interval of increased flux and calving, but for the moment, we will not change the timing of the forecast retreat as given in our Report#2, pending further information on the basin geometry.

3. Synthesis

In this section of the report, we provide a qualitative synthesis of the current and future status of the retreat, including an evaluation of the potential for future changes in iceberg hazards. While qualitative and somewhat speculative, our synthesis is a compilation of expert opinion, formed over decades of studying the retreat at Columbia Glacier. We adopt language used by the Intergovernmental Panel on Climate Change (IPCC) to assign likelihood in a consistent fashion. The probabilities listed in Table 1 are not determined by calculation, but are estimates of probability assigned to statements to calibrate distinctions such as “likely” vs. “very likely.”

Table 1. Likelihood Scale	
Term*	Likelihood of the Outcome
<i>Virtually certain</i>	99-100% probability
<i>Very likely</i>	90-100% probability
<i>Likely</i>	66-100% probability
<i>About as likely as not</i>	33 to 66% probability
<i>Unlikely</i>	0-33% probability
<i>Very unlikely</i>	0-10% probability
<i>Exceptionally unlikely</i>	0-1% probability

Table 1. IPCC uncertainty language (IPCC, 2013)

Two major shifts have occurred in the past decade in the characteristic calving flux and retreat rate of Columbia Glacier. The first shift, starting about 2006, was the release of the terminus from the constriction in the “Kadin-Great Nunatak Gap,” (K-G Gap) when the terminus started a rapid retreat across the deep basin at the West/Main branch confluence. Between ca. 2001 and 2006, the terminus had been in a state of quasi-stability in the K-G gap, when ice flux and calving rate were extremely high but retreat rate low. The second shift started in late summer 2010, when another quasi-stable terminus position was established at the upstream end of the overdeepened basin at the West/Main branch confluence. Since 2010, the ice speed has slowed relative to earlier periods during the retreat, probably in response to thinning and alterations in subglacial hydrology. Current conditions at the terminus - low surface slope, shallow water depths, and thinner ice (but still well about the threshold value for dynamic instability) – all point to continued stability relative to earlier epochs. Radar and model data both agree that the bed remains shallow (with water depths nowhere exceeding ca. 200 - 300 m) from its current position to the tidewater limit, with a number of subglacial pinning points that will anchor the glacier bed, reducing ice speed and along-flow extension, both of which will reinforce stability.

While further modeling and analysis will help to clarify details and reinforce confidence in our conclusions, we judge that the evidence and analysis to date indicates that calving rates during the remaining 14-20 years (duration is **very likely**) of Columbia Glacier’s retreat will fall below the levels observed during the 2006-2010 interval. The remaining retreat will **likely** be punctuated by short-lived (months to one year) episodes of increased flux and calving, but even during these episodes calving rates and berg size will **very likely** be less than the maximum values observed in the past.

Our analysis is informed by several data sources, several of which are discussed in detail above. TerraSAR-X radar interferometry provides measures of ice motion on the glacier. Ground-based time-lapse cameras help to fill velocity changes at finer spatial and temporal scales than are available from remote sensing. Several cameras placed at a variety of locations have been documenting changes in glacier motion, terminus position, and iceberg calving characteristics since 2004. Surface elevation on the glacier is derived from optical imagery (e.g. Worldview satellite) and airborne laser altimetry operated by the University of Alaska at Fairbanks. Model estimates of the glacier bed topography are given by McNabb et al., (2012), supplemented by airborne radio echo

sounding measurements (Rignot et al., 2013). The measurements show some important differences from the McNabb modeling, including the presence of thick ice and a marine-grounded basin on the East branch, located above the previously determined tidewater limit. However, further measurements are required to determine the effect this basin may have on future retreat (for example, whether the basin is closed or has a marine connection to the main forebay). Glacier seismicity as documented by The Alaska Earthquake Information Center (AEIC) also plays a role in our assessment. Their continuous monitoring of seismicity in Alaska shows that production of seismicity from Columbia Bay increased dramatically in late summer 2010, at the same time that the glacier terminus re-grounded and stabilized in shallow water. This is consistent with other regional observations, which show that glacier seismicity tends to be associated with tidewater glacier termini grounded in shallow water.

Our recent observations and analysis agree qualitatively with the best understanding of large-scale calving glacier behavior, as outlined, for example, by Amundson and Truffer (2010) and Post et al (2011). These papers describe how tidewater glaciers oscillate between “stable” and “very unstable” during the advance-retreat cycle, but rarely remain in quasi-stable, mid-retreat positions (as Columbia was in 2001-2006 and is now, to a lesser extent) for extended periods. While the retreat of Columbia Glacier terminus has slowed at various times since its onset in the early 1980s, other measures of retreat – rate of mass loss, for example – continued at high rates during these pauses, and nothing resembling a true return to stability has occurred. Long-term stability will be achieved only when the glacier retreats to the tidewater limit, where the bed rises above sea level. At the same time, as discussed above, calving and terminus retreat rates during the remainder of the retreat will **very likely** be smaller in magnitude than the larger episodes (e.g. during 2006-2010) in the past. Even though present-day dynamics are substantially reduced from previous levels, ice discharge remains elevated well above what would be considered stable. In its current state, Columbia Glacier remains one of Alaska’s fast-flowing, most rapidly changing glaciers in Alaska.

An outward sign of the trend toward stabilization is a change in the size and frequency of iceberg production. As stability increases, iceberg production becomes more frequent, uniform, and characterized by smaller bergs (reduced ice thickness at the calving terminus constrains the upper limit on iceberg size). Recent observations show this pattern. Estimates of ice flux to the terminus also support increasing stability. Ice delivery to the calving front has decreased by from peak values by at least a factor of 2, and calving rates are highly erratic (near stoppages of flow).

The final stages of our analysis are ongoing and involve completing the model representation of downfjord iceberg transport and passage over HBMS. Progress on this front is summarized in Appendix 1. Among the most significant factors influencing the fate of icebergs entering the forebay at the glacier’s retreating terminus is the increasing length of forebay and increasing water temperature, both of which exert first-order control on iceberg melt and degradation. Although data are spatially sparse for Prince William Sound, the GAK 1 Buoy near Seward shows a long-term warming trend. Given that fjord circulation involves density gradient driven or “baroclinic pumping” of water over the sill and circulating it inside the fjord, it is **likely** that ice cliff melting and

berg melting have increased and will continue to increase throughout the remainder of the retreat. Taken together with the reduced initial berg size, the probability of surviving the passage down the entire forebay and the size of icebergs that do make it all the way to HBMS are both declining. On the other hand, smaller mean berg size at HBMS will increase the fraction of bergs passing over the shoal and into Prince William Sound.

Growlers (icebergs with freeboard height of < 1 m) present one of the greatest hazards to shipping traffic, and are hard to detect with radar. Time lapse imagery shows a decrease in berg size from prior to 2006 to 2010, potentially suggesting that more small bergs could be escaping from the fjord. However, the effect of this change on berg sizes in Prince William Sound should have been apparent by now. Analysis of the SERV S ice radar reports may show whether this change was apparent in the tanker shipping lanes. Our top remaining research priorities include characterization of berg melt and degradation in the forebay and passage of bergs over HBMS. Ongoing work on these tasks is summarized in Appendix 1.

4. Summary

In this third report to the RCAC we include a qualitative but informed, expert synthesis of the retreat state. Our primary findings to date include:

- Ice concentrations inside the moraine are higher than expected, but the moraine continues to block most ice from exiting. Although Columbia Glacier still produces some of the larger bergs in the state, the extremely large calving events that were commonly produced in the early 2000s no longer occur due to shallow water conditions at and upstream of the present-day terminus. It is **very unlikely** that extremely large calving events will occur in the future.
- Several processes interact to reduce both the chances of iceberg survival all the way to HBMS and mean size of survivors at arrival at HBMS.
- A new region of ~1km thick ice, grounded in water 200-300 m deep, was discovered in the upper East branch. This ice does not have clear marine-grounded route of access to the forebay necessary to result in another rapid discharge episode, but it is **likely as not** that ice stored here will prolong the duration of overall retreat.
- Delivery of ice by glacier flow to the calving front is declining. We expect that future short-lived episodes of moderately increased flux are **likely**, but prolonged episodes and high calving fluxes are **unlikely** to return to historic levels.
- Time-stamped image sequences that were fundamental to building our understanding of current conditions are being delivered with this report.

Work continues on the more quantitative aspects of the assessment. In particular we continue to 1) develop a quantified iceberg-size distribution, 2) develop a downfjord iceberg-transport model 3) compile a self-consistent analysis of the long-term retreat including terminus position, velocity and geometry changes to identify mechanisms influencing the pace of retreat. The importance of continued funding for TerraSAR-X

imagery cannot be understated as these data ensure that we can continue to measure ice flux, and berg distributions at high space and time resolution in the future

Our work to date has illustrated some important processes ongoing at the Heather Island Moraine. Of particular importance is rapid uplift of the region that is apparent from sparse GPS observations. We are working on establishing a collaboration with UAFs Jeff Freymeuler to assess tectonic uplift. This will be introduced as a new component of the research during spring 2014.

5. References

- Amundson, J. M. & Truffer, M. A unifying framework for iceberg-calving models. *Journal of Glaciology* **56**, 822–830 (2010).
- Campbell, R.W. PWS Herring survey: Plankton and oceanographic observations. Exxon Valdez Oil Spill Restoration Project Final Report (Restoration Project 10100132A), Prince William Sound Science Center, Cordova, Alaska. (2013)
- Echelmeyer, K. A. & KAMB, B. Stress-gradient coupling in glacier flow. II: Longitudinal averaging in the flow response to small perturbations in ice thickness and surface slope. *Journal of Glaciology* **32**, 285–298 (1986).
- Kamb, B. *et al.* Mechanical and hydrologic basis for the rapid motion of a large tidewater glacier: 2. Interpretation. *J. Geophys. Res.* **99**, 15231 (1994).
- Kamb, B. & Echelmeyer, K. Stress-gradient coupling in glacier flow. I: Longitudinal averaging of the influence of ice thickness and surface slope. *Journal of Glaciology* **32**, 267–284 (1986).
- Kamb, B. & Echelmeyer, K. A. Stress-gradient coupling in glacier flow: IV. Effects of the 'T' term. *Journal of Glaciology* **32**, 342-349 (1986).
- Krimmel, R. M. Photogrammetric data set, 1957-2000, and bathymetric measurements for Columbia Glacier, Alaska. US Geological Water-Resources Investigations Report 01-4089 (2001).
- Hock, R., O'Neel, S. & Rasmussen, L. A. Using surface velocities to calculate ice thickness and bed topography: a case study at Columbia Glacier, Alaska, USA. *Journal of Glaciology* **58**, 1151–1164 (2012).
- Meier, M. F. and A. Post, Fast tidewater glaciers. *J. Geophys. Res.* **92**, 9051 (1987).
- Meier, M. *et al.* Mechanical and hydrologic basis for the rapid motion of a large tidewater glacier: 1. Observations. *J. Geophys. Res.* **99**, 15219 (1994).
- O'Neel, S., Pfeffer, W. T. & Krimmel, R. Evolving force balance at Columbia Glacier,

W.T. Pfeffer Geophysical Consultants, LLC

Alaska, during its rapid retreat. *J. Geophys. Res.* **110**, F3 (2005).

Post, A., O'Neel, S., Motyka, R. J. & Streveler, G. A complex relationship between calving glaciers and climate. *Eos, Transactions American Geophysical Union* **92**, 305 (2011).

Rignot, E. et al., Low-frequency radar sounding of temperate ice masses in Southern Alaska., *Geophys. Res. Lett.* (2013)

APPENDIX

Analysis and Materials Update

A1. Measuring iceberg distribution in the fjord

The most comprehensive source of information available about ice conditions throughout the full length of Columbia Bay is a series of high-resolution (1.8 meter pixel) TerraSAR-X images acquired on 11 to 22 day intervals since February 2011. Quantifying the distribution of icebergs as a function of distance from the terminus is a key first step towards developing a model of iceberg transport.

Results from our preliminary efforts to extract individual icebergs from the October 12, 2013 TerraSAR-X image are shown in Figure A1. As expected, iceberg size and density decline with distance from the terminus, the individual icebergs melting and fracturing on their journeys from the glacier terminus to the moraine shoal. Furthermore, the iceberg sizes follow a power law distribution, as predicted by percolation and particle models of ice calving (e.g. Bahr, 1995; Astrom et al., 2013).

Our image processing strategy, the results of which are shown in Figure 2A and 3A, leverages the brightness of ice and darkness of water in radar images, then makes additional assumptions about shape and texture to further filter the results. Particular care must be taken to not misinterpret swaths of mélange ice as huge individual icebergs.

Since iceberg production and transport cannot be assumed to be in steady state, results from one image are not necessarily representative, and we plan to repeat the same analysis over the full satellite time-series. Furthermore, since the 11 to 22 day time resolution is not sufficient to resolve the residence time of individual icebergs, the Heather Island (HI), Divider (AK10), and Kadin (AK01) time-lapse cameras will be used to estimate the residence time of icebergs in the fjord and couple instances of iceberg production at the terminus to iceberg transport over the moraine.

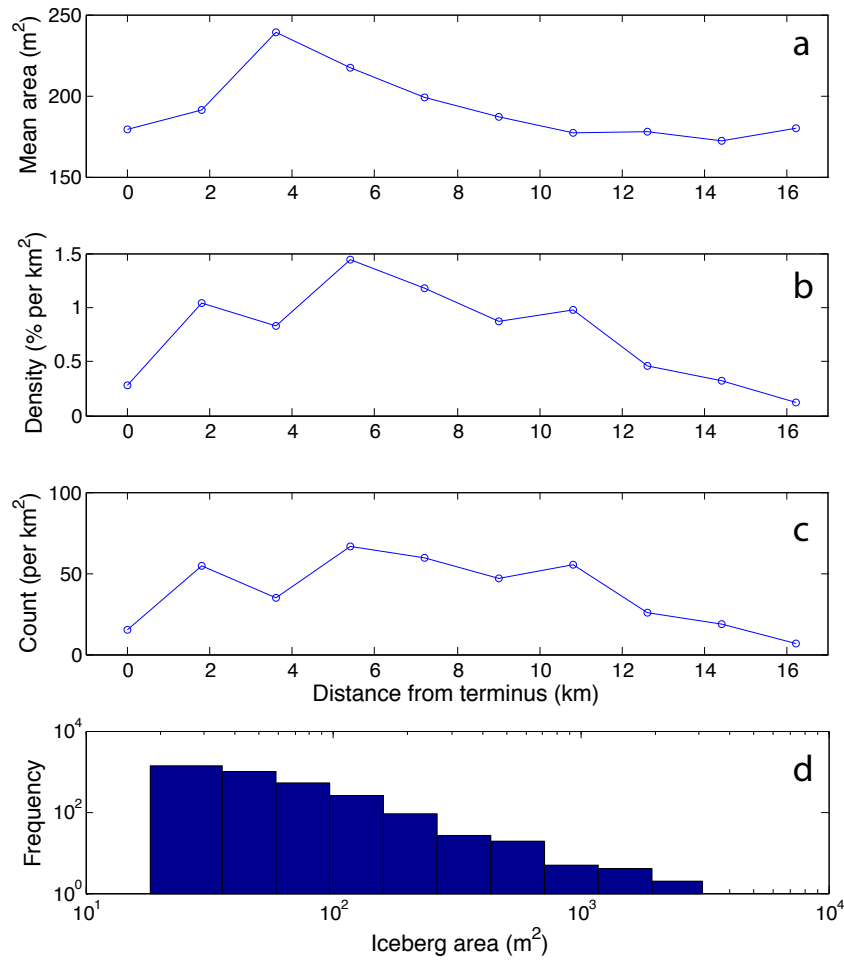


Figure A1. Summary statistics of Columbia Bay icebergs from the October 12, 2013 TerraSAR-X image: (a) mean iceberg surface area, (b) percent of fjord covered by icebergs, (c) number of icebergs per km^2 , and (d) log-log histogram of iceberg surface area.

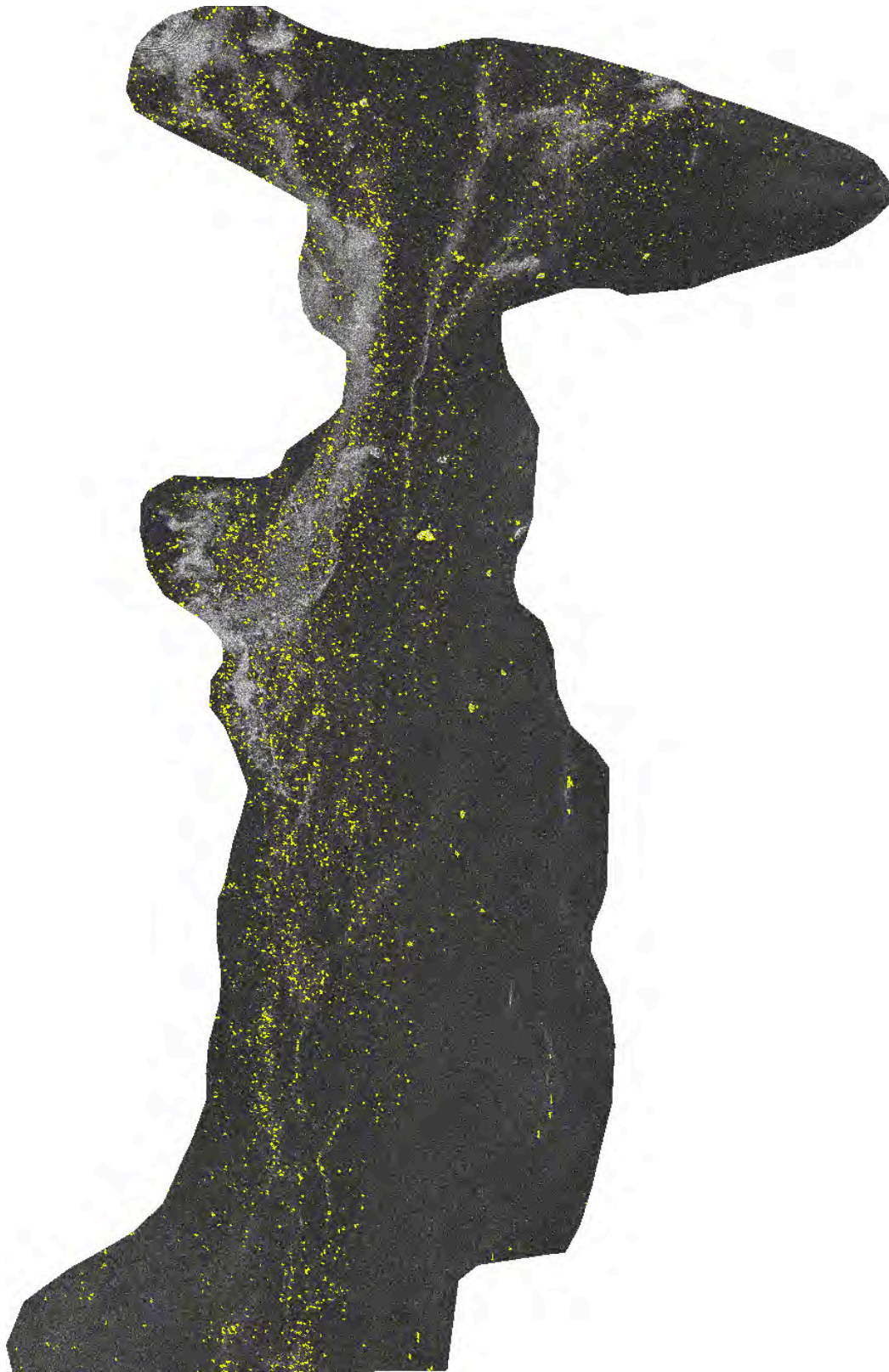


Figure A3. TerraSAR-X intensity image from October 12, 2013 overlaid with the boundaries of the icebergs detected by automated image processing.

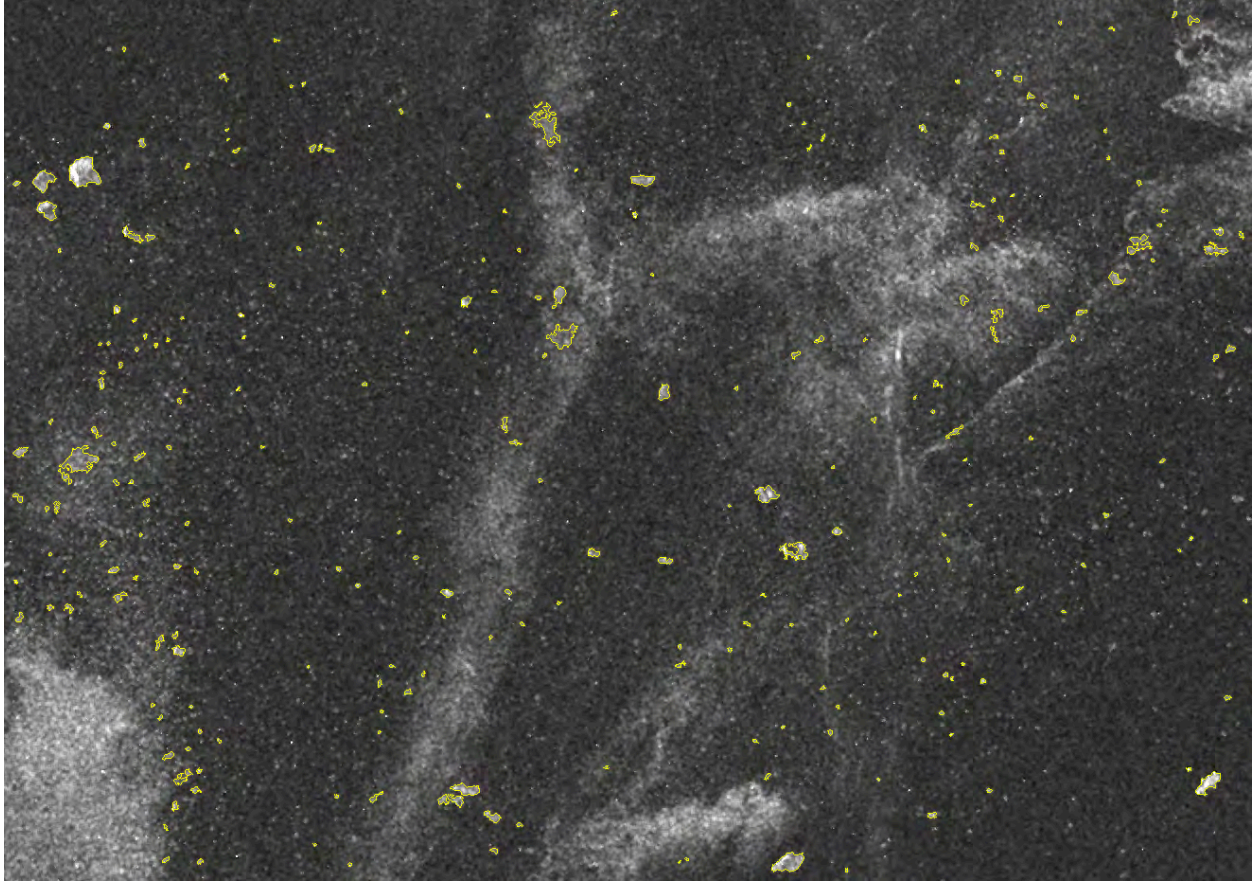


Figure A3. Detail view of the TerraSAR-X intensity image from October 12, 2013 showing the boundaries of the icebergs detected by automated image processing.

A2. Calving event size and time distributions

Over the course of 16 days in June 2005, Shad O'Neel and others watched the calving terminus of Columbia Glacier, recording the time, type, and magnitude of 828 individual events. Of these, 20 were photographed in such a way that the volume of calved ice could be estimated. The resulting size distribution is shown in Figure A4, and approximates a power-law distribution, suggesting that the calving process is scale-invariant. The glacier is capable of calving icebergs of all sizes, limited only to the size of the system itself, from small, frequent subaerial “avalanches” on the order of 100 m^3 to an enormous, very rare 10^8 m^3 event in which the entire terminus broke off at once (to this day the largest event ever observed at Columbia Glacier).

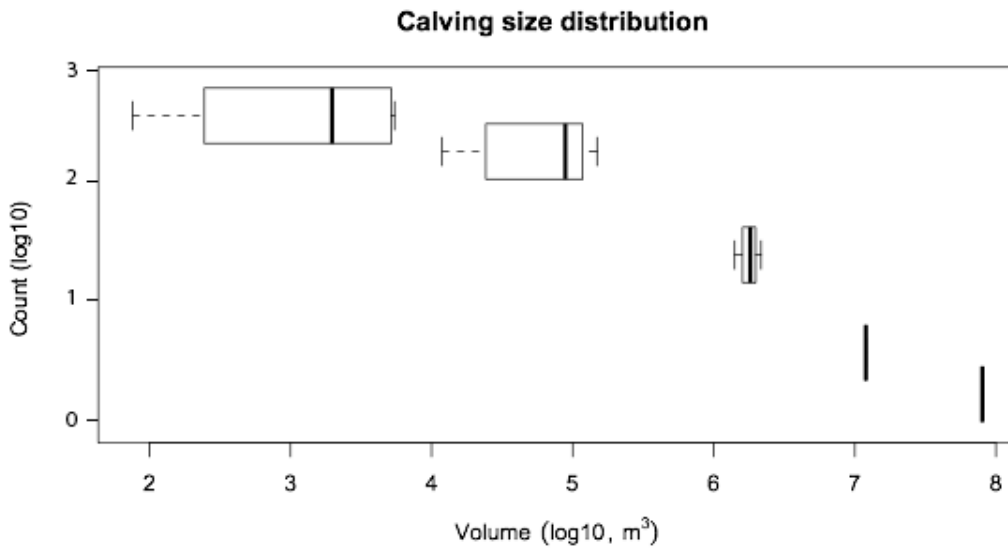


Figure A4. Calving event size distribution estimated from in-situ observations and photographs collected over 16 days in June 2005.

In 2005, the glacier was (just barely) grounded to the bed, a situation that the glacier finds itself in again presently, albeit with thinner ice and shallower water. By summer of 2009, much of the terminus was floating and the glacier reached its highest rate of *area loss* ever observed (as opposed to total *calving flux*). This transition from grounded to floating (and back to grounded) is illustrated in Figure A5.

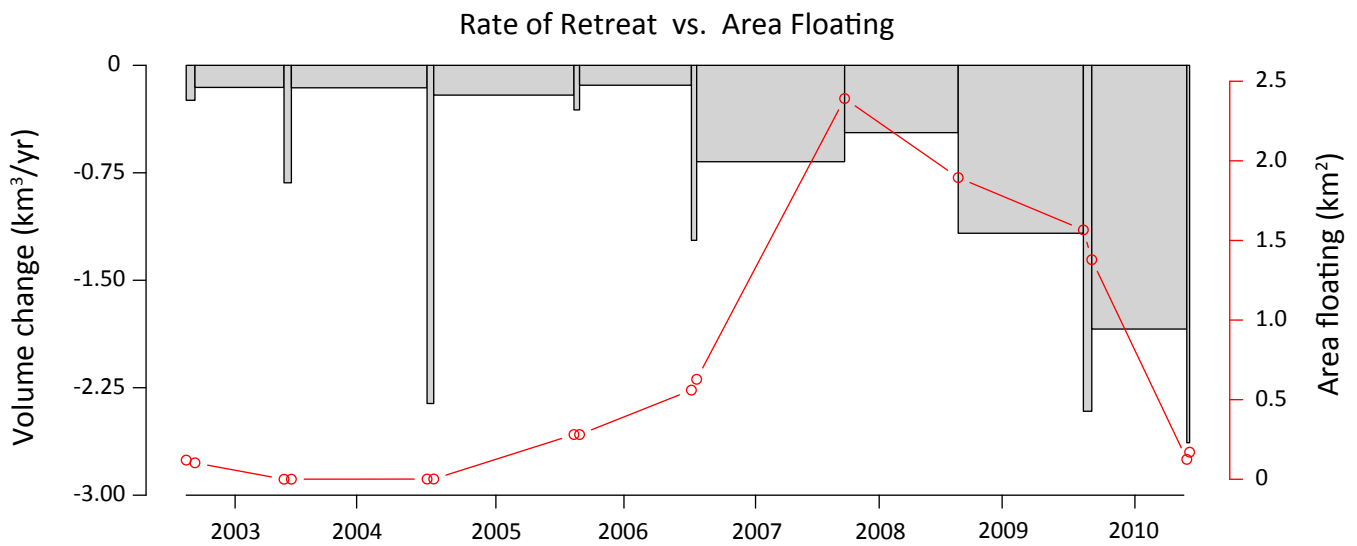


Figure A5. Increase in the rate of retreat following the transition from grounded to floating (and back to grounded) from 2003 to 2010.

As described in Walter et al. (2010), the transition marked a change in calving behavior, from smaller, more frequent calving events while grounded, to fewer and larger calving events while floating. The glacier's floating tongue disintegrated primarily through a sequence of enormous, tabular calving events.

In May to June 2009, a high-speed time-lapse camera was deployed, photographing the terminus every 45 seconds nearly continuously for 23 days – a sequence of 26,719 images ideal for resolving individual calving events. Comparisons of these two calving time-series, 2005 and 2009, confirm and build on our earlier understanding of the differences between the two regimes:

- Huge events were more than twice as frequent during flotation (2009) as they were when the glacier was grounded (2005), even though calving events were as little as half as frequent overall.
- Calving events in 2005 were 25% less likely to occur during low tide than during rising, high, or falling tide, a difference that disappeared in 2009. When the terminus is afloat, tide is expected to have little impact on stability, while when the terminus is very close to the flotation thickness ($dH \sim 10\text{m}$ in summer 2005), tide may matter more to calving. Figure A6 illustrates the significance of the tidal period to calving in 2005. Unfortunately, the series is not long enough to potentially resolve longer tidal periods. No peak is present in an equivalent analysis for 2009.
- The time between intervening calving events are, like the size distribution, found to approximate a power law (Figure A7). The results are very similar for both years, but suggest that shorter intervals were more common, and longer intervals less common in 2005, as expected.

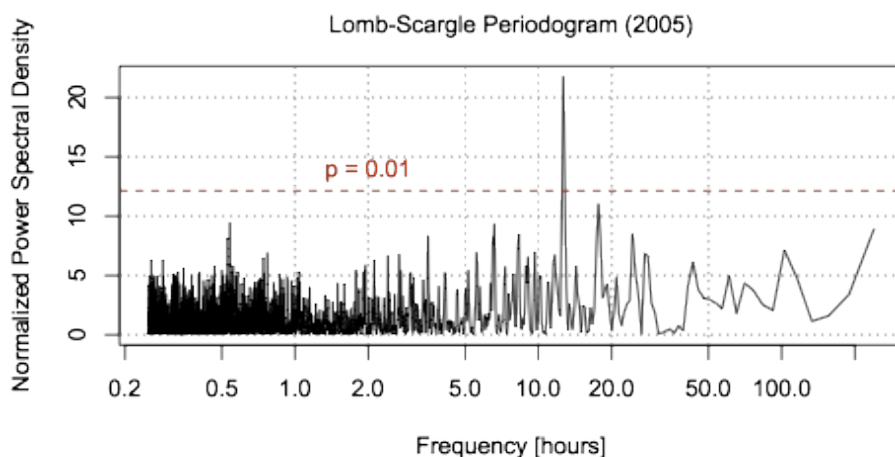


Figure A6. Lomb-Scargle periodogram of the 2005 calving time-series showing a statistically significant peak at 12.7 hours (0.529 days).

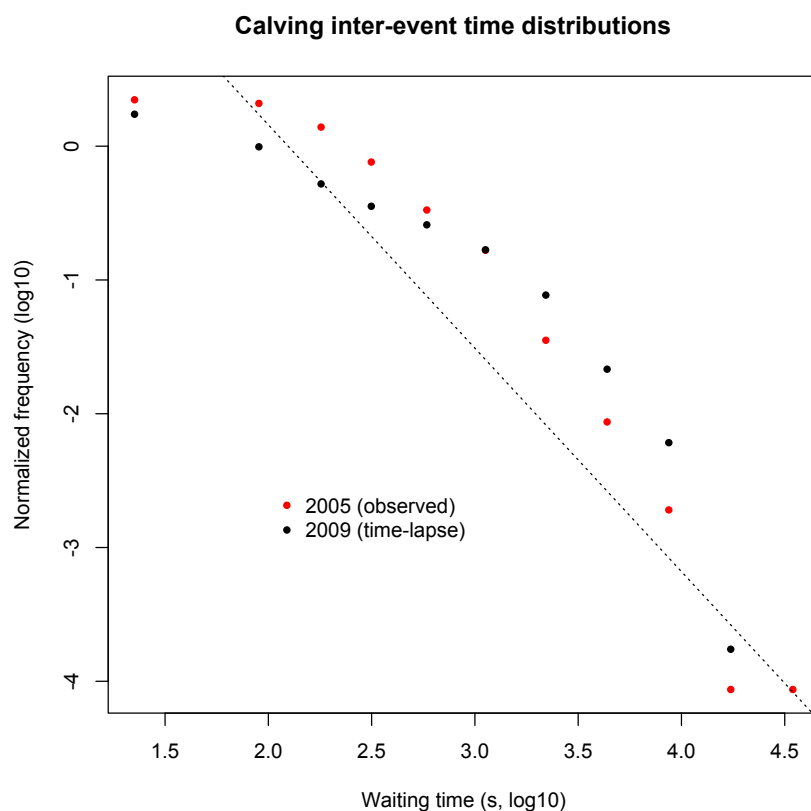


Figure A7. Distribution of inter-event waiting times between consecutive calving events at Columbia Glacier in summer 2005 (red) and summer 2009 (black). The dashed line represents the power law exponent (-1.67) predicted by the discrete particle model developed by Jan Astrom and other (2013). Comparisons between modeled and observed scaling laws in glacier calving are the subject of an upcoming paper O’Neel, Welty, and others are co-authoring with Astrom.

A3. Recovery of historic materials

In 1978-1985, a 16mm film camera maintained by the U.S. Geological Survey (under the direction of Robert M. Krimmel) photographed the glacier front once every hour for seven years (Krimmel and others, 1985). To our knowledge, this is the earliest time-lapse of a tidewater glacier ever produced, but sadly only a tiny fraction of the original film has been found. However, early-production 16mm reels of the video produced by the USGS from the time-lapse footage (which includes only the best frame from each day) have been recovered from both the USGS Washington Water Science Center in Tacoma and the Western Region Offices in Menlo Park, California. One of the best among these has been scanned at 2K (2,000 pixels wide) by Video Producer Don Becker at the USGS Federal Center in Denver, Colorado, paid for by a USGS digital archiving grant. For the first time, this remarkable sequence of images is available to us for analysis. Two of the digitized frames are shown in Figure A8.

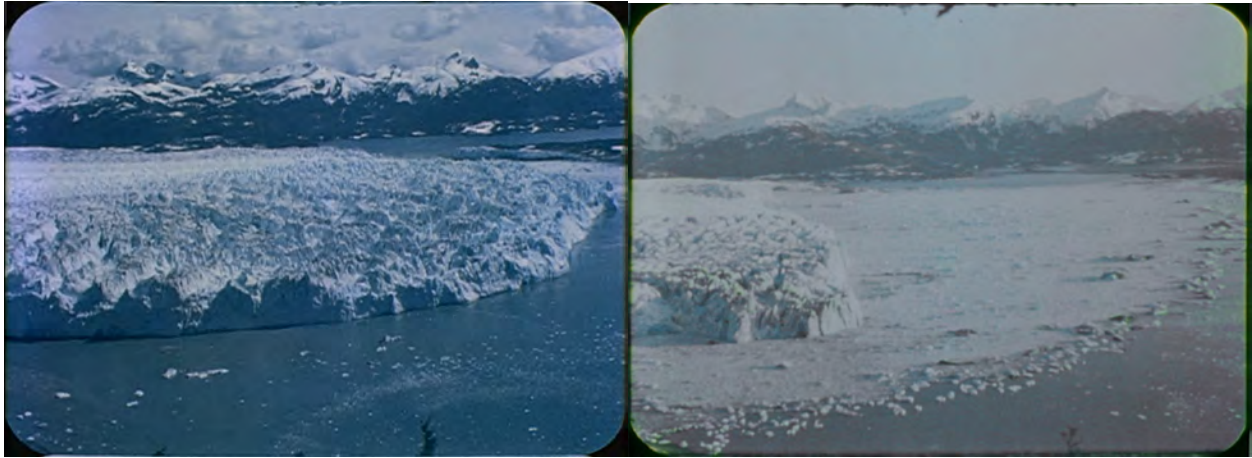


Figure A8. Example frames from the USGS time-lapse sequence, illustrating the onset of the retreat between 1979 and 1983.

References

- Åström, J. A., Riihilä, T. I., Tallinen, T., Zwinger, T., Benn, D., Moore, J. C., and Timonen, J. (2013), A particle based simulation model for glacier dynamics, *The Cryosphere*, 7, 1591-1602, doi:[10.5194/tc-7-1591-2013](https://doi.org/10.5194/tc-7-1591-2013).
- Bahr, D. B. (1995), Simulating iceberg calving with a percolation model, *J. Geophys. Res.*, 100(B4), 6225–6232, doi:[10.1029/94JB03133](https://doi.org/10.1029/94JB03133).
- Krimmel, R. M., Taylor, P., and Barber, P. (1985). *Time Lapse Observations of the Columbia Glacier, Alaska*. 16mm. Tacoma, Washington: U.S. Geological Survey.
- Walter, F., S. O'Neel, D. McNamara, W. T. Pfeffer, J. N. Bassis, and H. A. Fricker (2010), Iceberg calving during transition from grounded to floating ice: Columbia Glacier, Alaska, *Geophys. Res. Lett.*, 37, L15501, doi:[10.1029/2010GL043201](https://doi.org/10.1029/2010GL043201).